

## NUMERICAL ASPECTS FOR THE DYNAMIC SIMULATION OF THE FIXED-BED METHANOL SYNTHESIS TUBULAR REACTOR

Flavio Manenti<sup>1,\*</sup>, Silvia Cieri<sup>2</sup>, Marco Restelli<sup>2</sup>, Nadson Murilo Nascimento Lima<sup>3</sup>, Lamia Zuniga Linan<sup>3</sup>, Guillermo Durand<sup>4</sup>

<sup>1</sup> Politecnico di Milano, Dipartimento di Chimica, Materiali e Ingegneria Chimica “Giulio Natta”, Piazza Leonardo da Vinci 32, 20133 Milano, ITALY

\* [flavio.manenti@polimi.it](mailto:flavio.manenti@polimi.it)

<sup>2</sup> Novartis Vaccines & Diagnostics, Via Fiorentina 1, 53100 Siena, ITALY

<sup>3</sup> University of Campinas (UNICAMP), Department of Chemical Processes, PO Box 6066, 13081-970, Campinas, São Paulo, BRAZIL

<sup>4</sup> Planta Piloto de Ingeniería Química (UNS-CONICET), Camino La Carrindanga, Km. 7, 8000 Bahia Blanca, ARGENTINA

The purpose of this work is to develop a reasonably detailed dynamic model of a Lurgi-type industrial methanol synthesis reactor so as to determine important simplifications, to identify application/operating model limits, and to preliminary check the feasibility for the nonlinear model predictive control (NMPC) methodology. To do so, a partial differential equation (PDE) system is formulated and integrated to characterize the main phenomena occurring in this shell and tube boiler-reactor. The PDE numerical solution is performed through the use of several very performing algorithms (BzzMath library).

### 1. INTRODUCTION

Even though many improvements have been made since its first commercial implementation in 1923 and a series of new production technologies are being developed (Lange, 2001; Olah et al., 2009), methanol is still largely produced from natural gas, specifically via syngas (CO and H<sub>2</sub> mixture) obtained by means of steam reforming operations. Syngas is cooled and compressed before being sent to the reactor where reactants are mainly converted into methanol and water, and hence separated in an ad hoc process section. As the conversion is particularly low, unreacted gases are compressed and recycled to improve the efficiency of the process. As a result, a purge line must be considered to prevent any kind of accumulation of inert compounds.

The present paper focuses the attention on the dynamic modeling and control synthesis reactor of methanol from natural gas, via syngas (CO and H<sub>2</sub> mixture). The synthesis reactor is crucial to the overall process because of its intrinsic nonlinearity and the complex phenomena involved, especially in the fixed-bed Lurgi-type reactor (Lurgi GmbH, 2009) that we selected to be in line with the current trend for shell and tube reactor-boilers to be used in large-scale plants (Manenti et al., 2011a; Manenti et al., 2011b).

This special configuration sees the tube side filled with catalyst for the synthesis reactions, whereas the shell side is fed by water to regulate the reactor temperature and to generate high-pressure steam. For dynamics and control purposes, recent works developed by the authors (Manenti *et al.*, 2011a) highlighted that under normal operating conditions steady state description of the system is sufficiently defined by a pseudo-homogenous model (ODE) versus a more-detailed heterogeneous one (DAE). This leads to the development of a dynamic model of partial differential equations (PDE) system, traditionally hard to solve from a computational point of view (Logist et al., 2009). It is therefore necessary to implement a series of model formulations (parabolic and hyperbolic) and to investigate the computational effort required to integrate the dynamic model, especially looking forward the need of very high numerical performances for the implementation of a nonlinear model predictive control methodology (Manenti et al., 2009a; Viganò et al., 2010; Manenti, 2011) in the next works.

Please cite this article as: Manenti F., Cieri S., Restelli M., Nascimento Lima N.M., Zuniga Linan L. and Durand G., (2011), Numerical aspects for the dynamic simulation of the fixed-bed methanol synthesis tubular reactor, AIDIC Conference Series, 10, 223-232 DOI: 10.3303/ACOS1110025

## 2. MODELING

Methanol synthesis reactors are particularly hard to model as they involve at least four significant dimensions through which the system might evolve: (I) the axial direction of the reactor; (II) the radial direction of the reactor tubes; (III) the catalytic particle radius; and (IV) the time. However, when the research focuses principally on investigating the possibility to implement high time-computing CAPE (computer-aided process engineering) solutions such as nonlinear model predictive control, real-time dynamic optimization, and reactor hot-spot monitoring, the mathematical model is usually satisfactory to characterize the process transients if its axial behavior and the time evolution are well-simulated.

Accordingly, some simplifications and assumptions are reported below (Fogler, 1992; Levenspiel, 1999):

- Negligible axial diffusion: the PFR model is ideal. This hypothesis is removed in investigation of the process dynamics as discussed by Lovik and co-workers (Lovik et al., 1998).
- Negligible radial diffusion: concentration and temperature profiles are assumed as constant leading to a one-dimensional model.
- Constant radial velocity.
- Constant temperature and pressure profiles within the catalytic pellet (homogeneous catalytic particle).
- Negligible catalyst deactivation.
- Negligible side reactions, for the high catalyst selectivity (Moulijn et al., 2001; Hansen, 1997).

Moreover, according to Table 1, it is possible to completely characterize the methanol synthesis reactor through the definition of mass balances only for two compounds, water and methanol, being the mass fraction of the remaining species directly dependent on them: in fact, the rank of compounds/elements matrix is  $r = 3$  and two mass balance equations are enough to completely characterize the system.

Table 1: Compound-element matrix for the methanol synthesis

	$CO$	$CO_2$	$H_2$	$CH_3OH$	$H_2O$
$C$	1	1	0	1	0
$O$	1	2	0	1	1
$H$	0	0	2	4	2

It is not superfluous to remark that, as highlighted elsewhere (Manenti *et al.*, 2011a), even though the methanol yield is particularly small, the decrease in the number of moles across the reactor cannot be neglected.

## 3. DYNAMIC SIMULATION

The Plug Flow Reactor (PFR) model and the assumption of negligible axial diffusion lead to the development and time integration of the following dynamic model:

- Methanol:

$$\varepsilon_b \rho_{gas} \frac{\partial \omega_{CH_3OH}}{\partial t} = -\frac{M}{A_{int}} \frac{\partial \omega_{CH_3OH}}{\partial z} + MW_{CH_3OH} r_{CH_3OH} \quad (1)$$

- Water:

$$\varepsilon_b \rho_{gas} \frac{\partial \omega_{H_2O}}{\partial t} = -\frac{M}{A_{int}} \frac{\partial \omega_{H_2O}}{\partial z} + MW_{H_2O} r_{H_2O} \quad (2)$$

The energy balance results in:

$$\left[ \varepsilon_b \rho_{gas} c_{p_{mix}} + (1 - \varepsilon_b) \rho_{cat} c_{p_{cat}} \right] \frac{\partial T}{\partial t} = - \frac{M}{A_{int}} c_{p_{mix}} \frac{\partial T}{\partial z} + \pi \frac{U}{A_{int}} (T_{shell} - T) + \left[ r_{CH_3OH} (-\Delta H_{r_1}) + r_{H_2O} (-\Delta H_{r_2}) \right] \quad (3)$$

where:

$$r_{CH_3OH} = \rho_{cat} (1 - \varepsilon_b) \eta_1 (r_{CO \rightarrow CH_3OH} + r_{WGS}) \quad (4)$$

$$r_{H_2O} = \rho_{cat} (1 - \varepsilon_b) \eta_2 (r_{CO_2 \rightarrow CH_3OH} + r_{WGS}) \quad (5)$$

Kinetic laws and further information about parameters, operating conditions, and assumptions are the same already applied to solve the steady-state system (Manenti *et al.*, 2011a).

However, the integration of the dynamic PFR model results in certain numerical instabilities of the system, which are very far from the real physical behavior. The instability can be easily noted in Figure 1, reporting the trend of the reactor temperature profile at the 16th, 20th, and 80th seconds after having implemented a step-disturbance increase on the inlet flowrate temperature. This very stiff discontinuity that migrates across the reactor axis is due to the fact that the spatial node at the position  $n$ -th on the reactor axis has been integrated by using variables that have not yet been influenced by the perturbation, arrived to the  $(n-1)$ -th node only. After the dynamics imposed by the disturbance, the perturbed trend progressively overlaps to the original steady-state unperturbed trend.

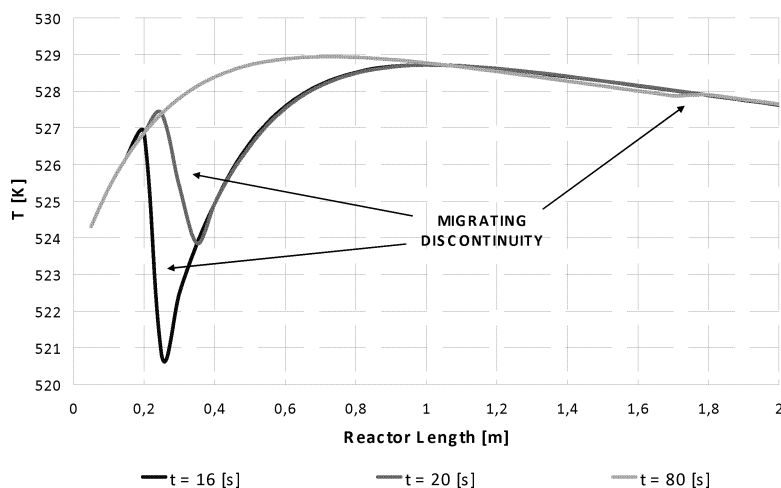


Figure 1: PFR model instabilities (Disturb on the  $T_{in}=523K$  at  $t=10s$ )

This migration and numerical instability is not only due to the flux segregation, which is typical of the ideal PFRs, but even to the methodology that we adopted to integrate the system: in fact, the finite-differences method here implemented exploits the previous incremental ratios (related to  $(n-1)$ -th variables at the  $t-1$  time interval); if the information needed by the numerical method is not yet achieved by the perturbation, the integration of all the subsequent nodes  $n, \dots, N$  is carried out as no perturbations were implemented. Consequently, the discontinuity migrates during the integration across the reactor profile by joining the perturbed trend to the original steady-state trend until the reactor dynamics is fully accomplished. The nodes that are the

interface between the perturbed and unperturbed trends generate the numerical discontinuity, which migrates from the beginning to the end of the reactor.

To remove the numerical instabilities, it is therefore necessary to eliminate the assumption of negligible axial diffusion and, thus, to introducing the diffusion term that we intentionally neglected in our previous paper on steady-state modeling of the methanol reactor (Manenti *et al.*, 2011a): the diffusivity can be assumed to be negligible for the steady-state modeling, but it must be accounted in the dynamic modeling of the fixed-bed methanol synthesis tubular reactor to prevent numerical instabilities. It is worth saying that many common numerical methods can easily fail in simulating the dynamics of this system if the diffusivity is neglected. Through the introduction of the diffusivity term, the resulting system is transformed from hyperbolic PDE to parabolic PDE. As one can see from the comparison of Figure 2, the instability problem reported in Figure 1 has been successfully solved.

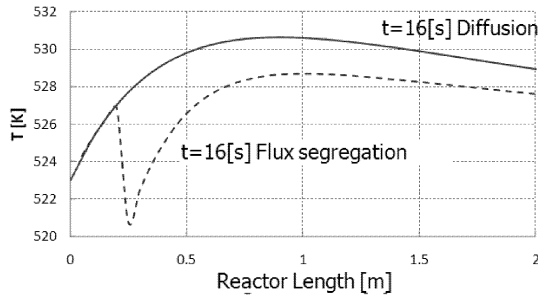


Figure 2: Ideal PFR (dashed) vs non-ideal reactor (solid)

According to the non-ideal formulation of the reactor, the model is provided in mass balances and the system assumes the following form:

– Methanol:

$$\varepsilon_b \rho_{gas} \frac{\partial \omega_{CH_3OH}}{\partial t} = -\frac{M}{A_{int}} \frac{\partial \omega_{CH_3OH}}{\partial z} + D \rho_g \frac{\partial^2 \omega_{CH_3OH}}{\partial z^2} + MW_{CH_3OH} r_{CH_3OH} \quad (6)$$

– Water:

$$\varepsilon_b \rho_{gas} \frac{\partial \omega_{H_2O}}{\partial t} = -\frac{M}{A_{int}} \frac{\partial \omega_{H_2O}}{\partial z} + D \rho_g \frac{\partial^2 \omega_{H_2O}}{\partial z^2} + MW_{H_2O} r_{H_2O} \quad (7)$$

The energy balance results in:

$$\begin{aligned} \left[ \varepsilon_b \rho_{gas} c_{p_{mix}} + (1 - \varepsilon_b) \rho_{cat} c_{p_{cat}} \right] \frac{\partial T}{\partial t} = \\ = k \frac{\partial^2 T}{\partial z^2} - \frac{M}{A_{int}} c_{p_{mix}} \frac{\partial T}{\partial z} + \pi \frac{U}{A_{int}} (T_{shell} - T) + \left[ r_{CH_3OH} (-\Delta H_{r_1}) + r_{H_2O} (-\Delta H_{r_2}) \right] \end{aligned} \quad (8)$$

#### 4. NUMERICAL STRATEGY

The method of lines is adopted for the numerical integration (Ozisik, 1994; Ullmann's, 2007). To prevent numerical discontinuities it is suitable to express the derivatives in their central form. By doing so, the system

cannot be integrated node by node, rather its overall structure is considered as the dependencies of the  $n$ -th node deal with both  $(n-1)$ -th and  $(n+1)$ -th nodes. The resulting Jacobian matrix assumes the diagonal-blocks structure with bands of Figure 3.

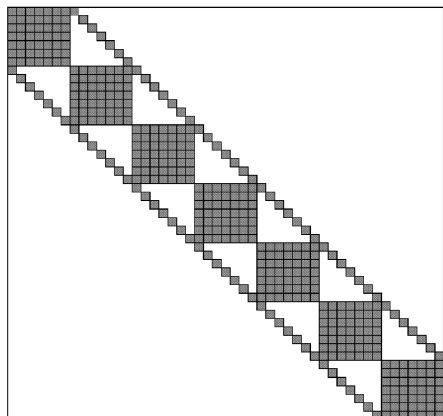


Figure 3: Jacobian qualitative structure. The number of diagonal blocks depends on the discretization across the reactor axis.

Such a structure entails the simultaneous solution of all nodes for each time interval (Buzzi-Ferraris and Manenti, 2010a). The class `BzzOdeSparseStiff` in `BzzMath` library (Buzzi-Ferraris, 2010) is adopted for its capability to exploit the matrix sparsity and the system structure so as to ensure fast computational times in spite of the complexity of the system we are solving. It is worth underlining that to solve the PDE system we adopted the central-differences discretization to transform the PDE into a series of ODE systems; hence, the Gear multivalued methods to handle stiff systems, the Newton methods to solve the related nonlinear algebraic system, and the linear system solvers (system factorization) for the linearized system are all implemented and ready-to-use for handling stiff problems in the `BzzOdeSparseStiff` class (Manenti and Rovaglio, 2008; Manenti et al., 2009b; Buzzi-Ferraris and Manenti, 2010a, 2010b; Manenti et al., 2011c).

We investigated both the parabolic and the hyperbolic PDE system by noting superior performances of the parabolic model: (I) it avoids non-physical oscillations generated by a first-order system; (II) the convection term can be approximated by using a forward formulation, leading to a more stable simulation; (III) more realistic solutions are obtained. For the sake of conciseness, we report parabolic model results only in the dedicated section.

#### 4.1 Adaptive Grids

After having opportunely coupled a detailed mathematical model for the methanol synthesis reactor with the most appropriate numerical methods to solve the resulting PDE system, the adaptive grids are also implemented to make the discretization denser where required (Figure 4) and sparser elsewhere. It is suitable to have a denser discretization in correspondence with the hot spot position so as to improve the estimation accuracy; thus a static upgrade is carried out to have more points in correspondence with the first 2 m of the reactor, whereas the grid is made sparser in the remaining 5 m in order to preserve the total amount of nodes and therefore to preserve the computational effort required to solve the system. By doing so, a better accuracy is obtained around the hot spot position in spite of the final part of the reactor, where process dynamics are less relevant than the ones occurring in the first 2 m.

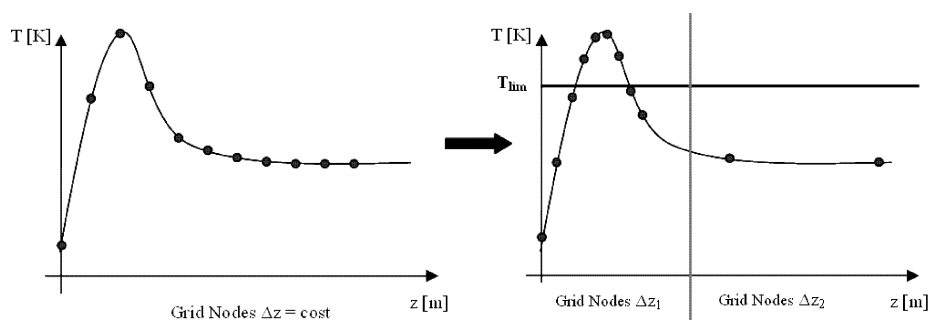


Figure 4: Qualitative scheme of adaptive grids aimed at making the profile characterization denser in correspondence with the temperature hot-spot.

## 5. RESULTS AND DISCUSSION

As stated above, the parabolic formulation of the PDE system leads to a diagonal-blocks matrix with bands; the introduction of the diffusive term (second order derivatives) allows to remove the non-physical oscillations generated by solving numerically the hyperbolic system (first order derivatives); in addition, it allows to approximate the convective term using a forward formulation to obtain a more realistic solution.

Once the model and the required solvers were properly implemented and validated and once the convergence of the overall system was opportunely checked, the open-loop dynamics generated by the perturbation of the most relevant parameters can be analyzed, leaving to future development the burden to close the loop and discuss the predictive control and dynamic optimization of the methanol synthesis reactor.

The parametric sensitivity is carried out by implementing a series of step disturbances on the following parameters: the shell temperature and the inlet mass flowrate of syngas.

By assuming that the syngas composition cannot be perturbed since it is directly fed to the methanol reactor as it exits the reformer, the system is particularly sensitive to the inlet feed flowrate. Figure 5 to Figure 6 report trends related to a variation of -50% in the mass flowrate of syngas entering the reactor. The reactor temperature profile of Figure 5 shows that such a decrease brings not only to a higher hot spot, from 528 K to 532 K, but also to a different hot spot position, from the original point in correspondence with 1 m to the new one in the neighborhood of 0.5 m (Figure 7).

It is worth underlining that the hot spot position is strictly related not only to the current methanol production as mentioned above, but even to the catalyst deactivation; thus, as the series of thermocouples could only roughly identify the hot spot positioning, it should be important to have a reasonable inference of the same hot spot and eventually to be able to control it and intentionally move it along the reactor in order to have a realistic measurement of it, in order to avoid or, ultimately, to “drive” catalyst deactivation (Figure 8).

The hot spot value increases and its upstream migration are motivated by the fact that the thermal hold-up to heat the fresh feed is evenly halved with the decrease of the feed flowrate.

The fast achievement of the hot spot, coupled with the fast decrease of temperature immediately after it, is the best condition for the methanol production as testified by Figure 6, showing that the methanol yield overcomes the 7% by undergoing these conditions. On the other hand, the overall production is practically halved.

Figure 9 and Figure 10 show the system answer to a feed flowrate increase by 50%. Hence, the temperature profile of Figure 9 progressively changes by reducing the hot spot and by migrating it forward along the axis. Also, after the hot spot the fluid phase temperature is gradually increased against the original steady-state. As a consequence, even though the overall production is improved because of the large process flowrate, the final methanol yield drops down the 6%.

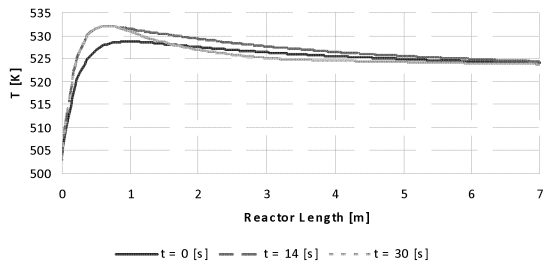


Figure 5: 50% decrease in the syngas inlet flowrate - Temperature profile

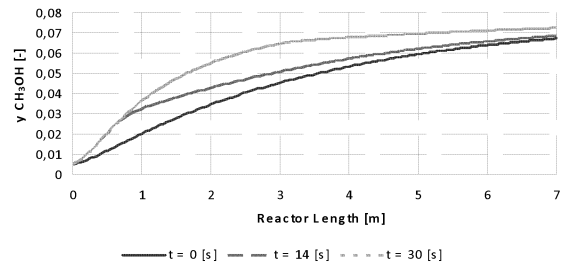


Figure 6: 50% decrease in the syngas inlet flowrate - Methanol profile

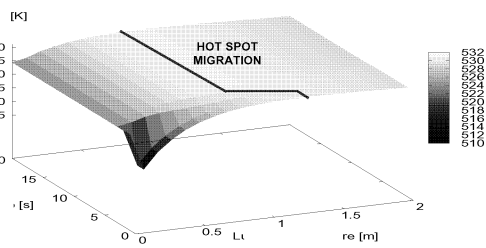


Figure 7: Hot spot migration

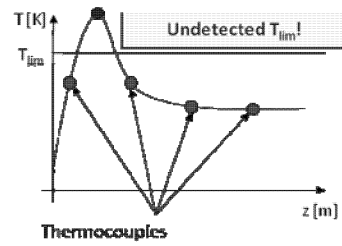


Figure 8: Undetected  $T_{lim}$  due to hot spot migration and thermocouples positioning

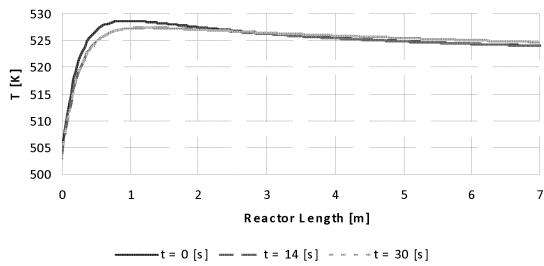


Figure 9: 50% increase in the syngas inlet flowrate - Temperature profile

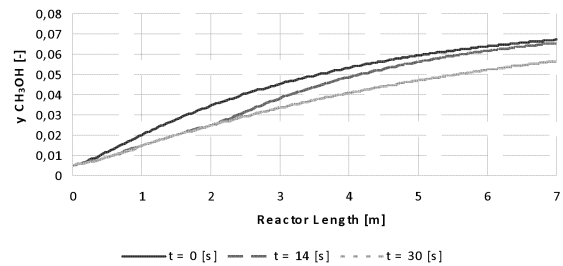


Figure 10: 50% increase in the syngas inlet flowrate - Methanol profile

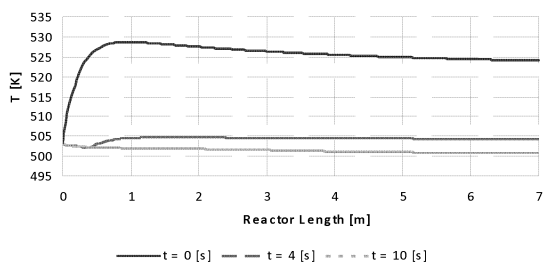


Figure 11: 50% decrease in the  $T_{shell}$  (-20K) - Temperature profile

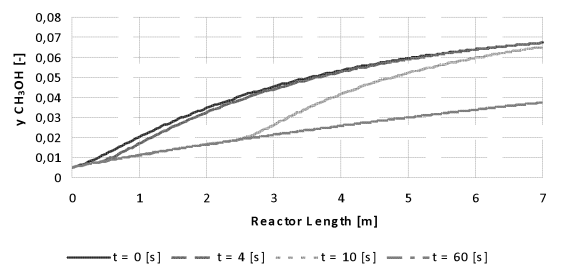


Figure 12: decrease in the  $T_{shell}$  (-20K) - Methanol profile

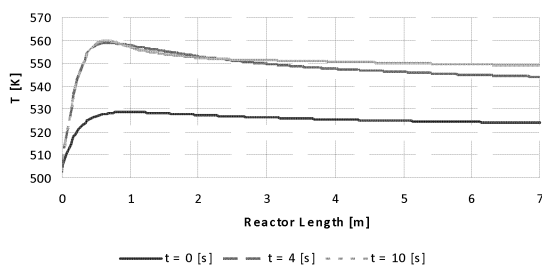


Figure 13: increase in the  $T_{shell}$  (+20K) - Temperature profile

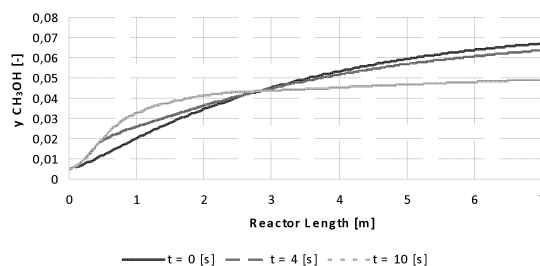


Figure 14: increase in the  $T_{shell}$  (+20K) - Methanol profile

Figure 11 to Figure 14 demonstrate that the system is more sensitive to any variation at the shell side temperature. Hence, the shell side of the reactor operates as a boiler for steam generation and the shell side temperature can be regulated either by directly measuring and regulating the water temperature or by managing the shell side pressure as the water within the shell side is at the equilibrium condition. This latter alternative is preferable even to efficiently regulate the steam pressure according to the power supply required by the joined facilities.

A variation of the shell side temperature in the order of -20 K inhibits the methanol conversion as the reactor is practically switched off. In fact, it is possible to see that the temperature profile of Figure 11 along the reactor drops from 525 K and with a hot spot of 528 K down to 502 K and the hot spot is vanished.

The dissipation of reaction heat is very fast for the combination of the immediate slow down of kinetics (in such operating conditions the conversion to methanol of the inlet flowrate is minimum) and the efficient heat exchange between shell and tube sides. The overall reactor is cooled in few seconds. The fast reduction of the reactor temperature has significant and evenly fast effects on the outlet mass fractions of Figure 12. The methanol production is kept competitive (methanol fraction equal to 6.8%) for about 5-6 s only after the implementation of the disturbance occurring at  $t = 3$  s, just the time needed to switch off the reactor, before dropping down to 3.8%.

As the system is so sensitive to the shell side temperature, it is interesting to investigate even the opposite variation, where the parameter is significantly larger than the design one. In this case, it is possible to see an inversion of the reactor temperature profiles (Figure 13). The reactor temperature practically immediately moves close to the new shell side temperature by preserving the original profile, whereas few seconds later the inversion of profile occurs. Such an inversion in the temperature profile is inevitably remarkable in the fraction profiles of Figure 14. It is worth noting that the methanol production is significantly reduced at the end of the reactor even though it is largely increased in the first meter of the reactor and specifically up the achievement of hot spot position. This is because kinetics behind the model is favored before the hot spot, whereas the remaining portion is governed by thermodynamic equilibrium that is penalized, being the reaction exothermic.

The step disturbances here assumed are intentionally hard to measure the computational effort under high dynamics regime. It is remarkable the computational time reduction obtained by introducing the diffusive term and moving from a first order to a second order PDE system: CPU times to simulate 100s under the same perturbation of Figure 11 and Figure 12 on an Intel® Core2™ Quad, 2.85 GHz, 3.0 GB RAM; Windows XP™ SP3; Visual Studio 6.0 are 78.02 s with first-order derivatives and 36.23 s with second order derivatives. The reason is the same mentioned above: diffusive term allows to stabilize the system reducing non-physical oscillations. Very efficient differential solvers (BzzOdeSparseStiff of BzzMath Library) allow taking benefit of matrix sparsity and structure, contributing to computational time reduction in a determining way, especially looking forward the implementation of nonlinear model predictive control methodology. In addition, the



proposed model fits satisfactorily well several sets of industrial data previously reconciled using robust data reconciliation techniques, which are described elsewhere (Signor et al., 2010).

## 6. CONCLUSIONS

A reasonably detailed dynamic model for the Lurgi-type shell and tube reactor-boiler for methanol synthesis has been described. An investigation on the most appealing numerical methods has been performed, showing that a good efficiency is obtained in the numerical integration of the parabolic formulation of the model, unlike the hyperbolic one, especially for the resulting diagonal-blocks with bands structure of the Jacobian obtained after the discretization across the reactor axis: despite of an increase in problem dimensionality, the matrix sparsity and structure have been both exploited efficiently by the implementation of ad hoc solvers. Also, the selection of proper assumptions in the dynamic modeling of the system allows overcoming possible numerical instabilities. The reduced CPU times gives the possibility, as future work, to implement the nonlinear model predictive control methodology on the Lurgi-type shell and tube boiler-reactor.

## NOMENCLATURE

$A_{int}$	Internal area of the tube	$[m^2]$	$r_{WGS}$	Reaction rate Water Gas Shift	$\left[\frac{mol}{s \cdot kg_{cat}}\right]$
$a_v$	Specific surface area of the catalytic pellet	$\left[\frac{m^2}{m^3_{cat}}\right]$	$r_{CO \rightarrow CH_3OH}$	Reaction rate methanol from carbon monoxide	$\left[\frac{mol}{s \cdot kg_{cat}}\right]$
$c_{p_{mix}}$	Specific heat of gas at constant pressure	$\left[\frac{J}{kg \cdot K}\right]$	$r_{CO_2 \rightarrow CH_3C}$	Reaction rate methanol from carbon dioxide	$\left[\frac{mol}{s \cdot kg_{cat}}\right]$
M	Mass flowrate	$\left[\frac{kg}{s \cdot tube}\right]$	$\epsilon_b$	Void fraction of catalytic bed	$[-]$
MW <sub>i</sub>	Molar weight of i-th component	$\left[\frac{kg_i}{kmol_i}\right]$	$\Delta H_j^{react}$	Enthalpy of j-th reaction	$\left[\frac{J}{mol}\right]$
T	Temperature of the gas phase	$[K]$	$\eta_j$	Reaction j-th efficiency	$[-]$
$T_{shell}$	Temperature of the shell-side of the reactor	$[K]$	$\rho_{cat}$	Density of the catalytic pellet	$\left[\frac{kg_{cat}}{m^3_{cat}}\right]$
U	Overall heat transfer coefficient	$\left[\frac{W}{m^2 \cdot K}\right]$	$\rho_{gas}$	Density of the gas phase	$\left[\frac{kg}{m^3}\right]$
Z	Axial coordinate	$[m]$	$\omega_i$	Mass fraction of component i in the gas phase	$[-]$

## REFERENCES

- Buzzi-Ferraris, G., & Manenti, F., 2010a, Fundamentals and Linear Algebra for the Chemical Engineer: Solving Numerical Problems. Wiley-VCH, Weinheim, Germany.
- Buzzi-Ferraris, G. (2010). BzzMath: Numerical library in C++. Politecnico di Milano, <http://chem.polimi.it/homes/gbuzzi>.

- Buzzi-Ferraris, G., & Manenti, F., 2010b, Interpolation and Regression Models for the Chemical Engineer: Solving Numerical Problems. Wiley-VCH, Weinheim, Germany.
- Fogler, H.S., 1992, Elements of Chemical Reaction Engineering. Englewood Cliffs, NJ, Prentice-Hall, US.
- Lange, J.P., 2001, Methanol synthesis: a short review of technology improvements. *Catalysis Today* 64(1-2), 3-8.
- Levenspiel, O., 1999, Chemical Reaction Engineering. 3rd Ed., Wiley, US.
- Logist, F., Saucez, P., Van Impe, J., & Vande Wouwer, A., 2009, Simulation of (bio)chemical processes with distributed parameters using Matlab. *Chemical Engineering Science*.
- Lovik, I., Hillestad, M., & Hertzberg, T., 1998, Long term dynamic optimization of a catalytic reactor system. *Computers & Chemical Engineering* 22, S707-S710.
- Lurgi GmbH, 2009, Lurgi MegaMethanol®. [www.lurgi.com](http://www.lurgi.com).
- Manenti, F., Cieri, S., & Restelli, M., 2011a, Considerations on the steady-state modeling of methanol synthesis fixed-bed reactor. *Chemical Engineering Science* 66(2), 152-162.
- Manenti, F., Cieri, S., Restelli, M., Lima, N.M.N., & Zuniga Linan, L., 2011b, Dynamic Simulation of Lurgi-type Reactor for Methanol Synthesis. *Chemical Engineering Transactions* 24, 379-384.
- Manenti, F., Buzzi-Ferraris, G., Dones, I., & Preisig, H.A., 2009a, Generalized Class for Nonlinear Model Predictive Control Based on BzzMath Library. *Chemical Engineering Transactions* 17, 1209-1214.
- Manenti, F., 2011, Considerations on Nonlinear Model Predictive Control Techniques. *Computers & Chemical Engineering*, 35(11), 2491-2509.
- Manenti, F., & Rovaglio, M., 2008, Integrated multilevel optimization in large-scale poly(ethylene terephthalate) plants. *Industrial & Engineering Chemistry Research* 47(1), 92-104.
- Manenti, F., Dones, I., Buzzi-Ferraris, G., & Preisig, H.A., 2009b, Efficient Numerical Solver for Partially Structured Differential and Algebraic Equation Systems. *Industrial & Engineering Chemistry Research* 48(22), 9979-9984.
- Manenti, F., Buzzi-Ferraris, G., Pierucci, S., Rovaglio, M., & Gulati, H., 2011c, Process Dynamic Optimization Using ROMeO. *Computer Aided Chemical Engineering* 29, 452-456.
- Olah, G.A., Goeppert, A., & Surya Prakash, G.K., 2009, Beyond Oil and Gas: The Methanol Economy. Wiley-VCH, Weinheim, Germany.
- Ozisik, M.N., 1994, Finite Difference Methods in Heat Transfer. CRC Press.
- Signor, S., Manenti, F., Grottoli, M.G., Fabbri, P., Pierucci, S., Sulfur Recovery Units: Adaptive Simulation and Model Validation on Industrial Plant, *Industrial & Engineering Chemistry Research*, 49(12), 5714-5724, 2010
- Ullmann's, 2007, Modeling and Simulation. Wiley-VCH, Weinheim, Germany.
- Viganò, L., Vallerio, M., Manenti, F., Lima, N.M.N., Zuniga Linan, L., & Manenti, G., 2010, Model Predictive Control of a CVD Reactor for Production of Polysilicon Rods. *Chemical Engineering Transactions* 21, 523-528.